ISBN: 978-3-95450-234-9 ISSN: 2673-5504 doi:10.18429/JACoW-SRF2023-WEPWB111

A NEW ULTRA-HIGH VACUUM FURNACE FOR SRF R&D

M. Wenskat[1,*], R. Ghanbari[1], C. Bate[1,2], C. Martens[1], W. Hillert[1]
[1]Universität Hamburg, Germany
[2]Deutsches Elektronen-Synchrotron DESY, Germany

Abstract

A new vacuum furnace has been designed and purchased by the University of Hamburg which is operated in an ISO5 cleanroom. This furnace can anneal single-cell TESLA cavities at temperatures up to 1000 °C and achieves a base pressure of 2×10^{-8} mbar at room temperature after 8 h of pumping. We lay out the underlying design ideas, based on the gained experience from our previous annealing research, and present the commissioning of the furnace itself. Additionally, we will show the first results of sample and cavity tests after annealing in the furnace.

DESIGN CONSIDERATIONS

Based on the experience gained with our vacuum heat treatments and from partner laboratories, we made some layout decisions. All studies indicate that the CO/CO_2 partial pressure levels are crucial for successful treatments [1–4]. Hence, an oil-free vacuum system was designed. Furthermore, a combination of a turbomolecular (TMP) and a cryopump was chosen to achieve the highest pumping speed for hydrogen and water vapor. In addition, to enable a partial pressure operation with the TMP but to avoid a backflow from roughing pumps, a by-pass solution was chosen. This will also allow the operation of a residual gas analyzer (RGA) during partial pressure operation. The furnace itself is vented or operated in partial pressure by bottled 6.0 nitrogen. The whole furnace was planed to be all-metal sealed (except the door) and only molybdenum heaters and heat shields were used. The total gas flow q_{pV} at ultimate pressure was specified to be better than 5×10^{-4} mbarl/s and the overall leak rate Q_L better than 1×10^{-9} mbarl/s. Also, the cooling water can be heated up to 80 °C, which is used prior to opening the furnace to minimize the adsorption of water to the inner furnace walls. The final layout of the furnace is given in Fig. 1. After discussing the specifications with several companies, the company *Xerion Berlin Laboratories® GmbH* had the most convincing concept and built the furnace. The furnace is a bottom loader, capable to fit a 1.3 GHz TESLA single-cell cavity inside, see Fig. 2. The furnace vessel is made out of 1.4301 stainless steel and has electropolished inside surfaces. The maximum achievable temperature is 1100 °C, with a homogeneity of ±5 °C and is controlled by three heating zones. The furnace is located in a clean room (ISO 5) to minimize particle contamination.

COMMISSIONING

Test runs were carried out at varying temperatures and durations. The ultimate pressure achieved after several days

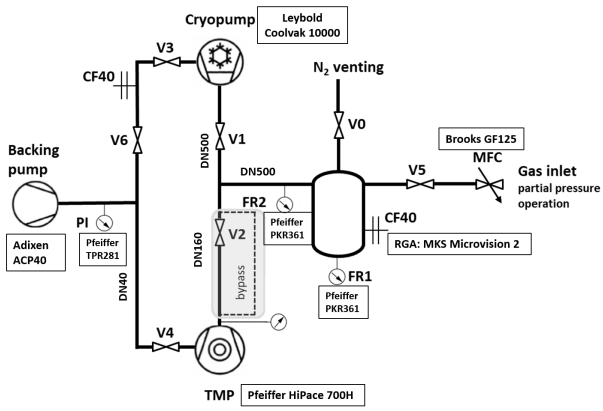

Figure 1: Layout of the vacuum system.

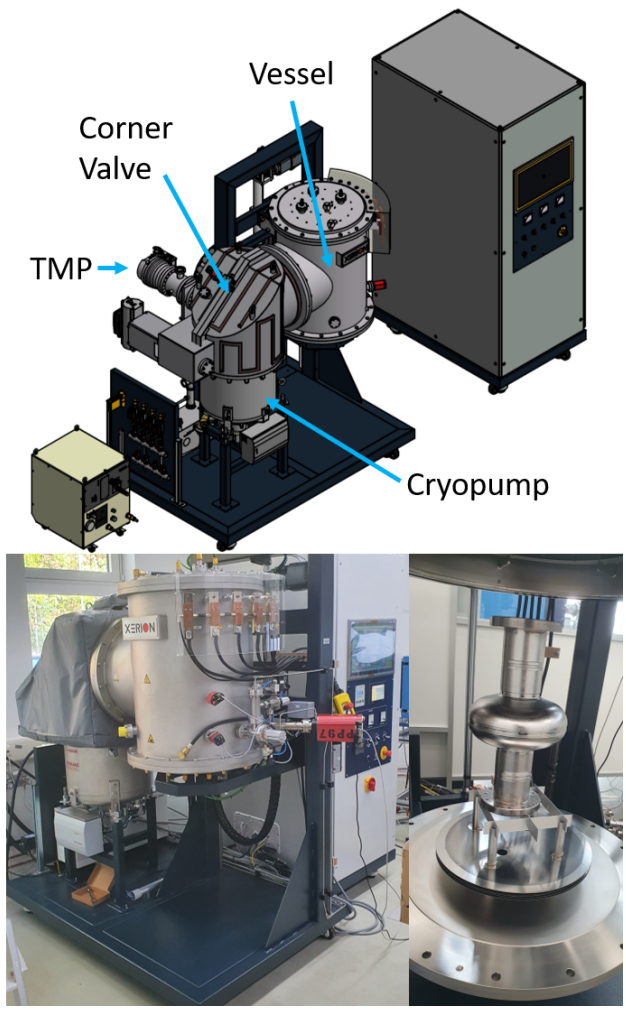

Figure 2: *Top*: CAD drawing of furnace. *Bottom left*: Image of the furnace before cleanroom installation. *Bottom right*: Single-cell cavity 1DE10 installed in the open furnace.

* marc.wenskat@desy.de

ISBN: 978-3-95450-234-9 ISSN: 2673-5504 doi:10.18429/JACoW-SRF2023-WEPWB111

of pumping is better than 2×10^{-9} mbar (limited by the resolution of the pressure gauge), and the corresponding RGA at room temperature (RT) is shown in Fig. 3.

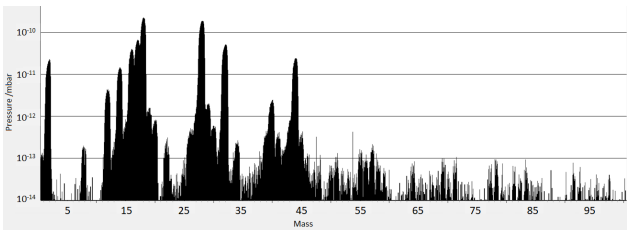

Figure 3: RGA taken at room temperature.

The regular start pressure for any heat treatment is better than 2×10^{-8} mbar which is achieved after 8 h pumping. This pressure is desorption limited by hydrocarbons degassing from the furnace wall when the water heating is turned on, resulting in a RGA as shown in Fig. 4. The absolute pressure

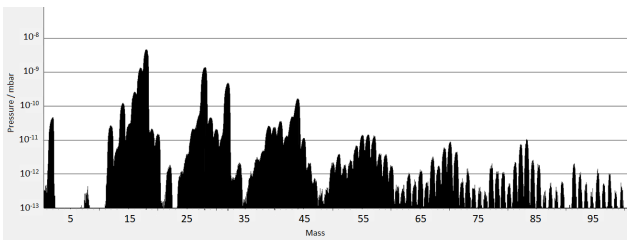

Figure 4: RGA taken at room temperature with furnace walls at approximately 60 °C due to water heating.

values of the masses above 45 at RT are in the range of 1×10^{-11} mbar or better and the source of this pollution was unclear.

During a 900 °C run planed for 10 h, a warning in the control system regarding the end position of the corner valve closing the cryopump, accompanied by a pressure spike up to 1×10^{-4} mbar, occurred after approximately 8.5 h. As the corner valve was closed during this run and the whole furnace was pumped only with the TMP, it was unclear why the endswitch caused an error signal although the valve plate was in position. After a detailed analysis, a wrongfully installed component was found to be the origin. The shaft was glued instead of welded to the lever which lifts and closes the valve plate. During the long annealing run, the lever heated up until the glue vaporized, causing the pressure spike. Loosing the connection to the lever, the shaft rotated further, causing the endswitch to signal the missing endposition. Hence a major contribution, possibly the only, to the hydrocarbon contamination of the furnace can be linked to a glued connection.

After a disassembly and exchange of the faulty component, a manual cleaning of the corner valve and several cleaning annealings have been done. The following studies were done after this process and describe the furnace in its current state.

Furnace Vacuum Studies

A leak search using a *Pfeiffer Vacuum ASM340* leak detector showed no leak above $Q_L = 10^{-10}$ mbar l/s. To get a first estimate of the total gas load, one can use the pumping speed S of the vacuum pump used and multiply it with the pressure achieved with that pump to obtain the throughput q_{pV} of that vacuum pump. From a conservation point of view, this has to be equal to the gas load from the furnace, including all contributions such as desorption, permeation and leaks. With water heating turned on, this yields for the TMP to $q_{pV} = 1.2 \times 10^{-4}$ mbar l/s and for the cryopump to $q_{pV} = 1.8 \times 10^{-4}$ mbar l/s for the furnace. Both numbers agree well with each other. If the water heating is turned off, the ultimate pressure drops by an order of magnitude for the cryopump, and so does q_{pV} to 2×10^{-5} mbar l/s

It is further possible to obtain the desorption rate Q_{des} from the curve of rising pressure when all vacuum pumps are turned off. Plotted on a graph with linear scales, the pressure rise must be a straight line. If the increase is dominated by desorption, as expected here from the small leak rate Q_L, then this pressure rise will taper off after a certain time and will approach an equilibrium value. This is motivated by the fact that over time, the coverage rate of the surface decreases. The procedure for the rate-of-rise test was as follows: (i) turn off water heating and evacuate the furnace with the TMP for 12 h (ii) then further evacuate the furnace with the cryopump for another 8 h. After that duration all valves are closed. The pressure in the furnace was monitored continuously as shown in Fig. 5.

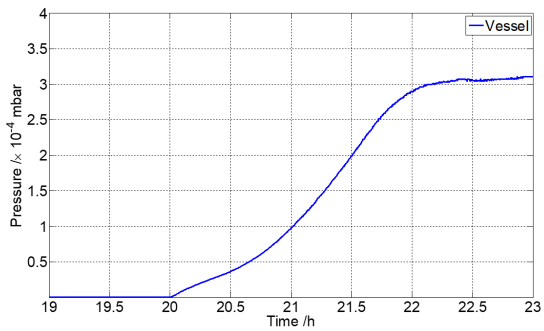

Figure 5: Pressure vs. time for the vessel. A tapering off is obvious.

A good approximation of the desorption rate can be obtained by assuming that after a given point in time $t > t_0$, the rise will behave linear over time, where t_0 is typically assumed to be 1 h. Fitting a linear curve to the pressure rise after 1 h results in a rate of 5.8×10^{-8} mbar/s. With the total furnace volume, the desorption rate is calculated to $Q_{des} = 1.16 \times 10^{-5}$ mbar l/s. This value agrees well to the above derived q_{pV} for the case with cryopump turned on and the water heating turned off. It further supports the assumption that the gas load is dominated by desorption and not by a leak, and that the water heating increases the desorption of hydrocarbons from the furnace walls, as also seen in the RGA.

ISBN: 978-3-95450-234-9 ISSN: 2673-5504 doi:10.18429/JACoW-SRF2023-WEPWB111

We can also compare this to the material specific desorption flow density q_{des} of the used materials. The furnace surface is approx. 9.8 m^2, which then yields a desorption flow density of $q_{des} = 1.18 \times 10^{-10}$ mbar l/cm^2 s. This value is in good agreement with the typical rate of unbaked austenitic steels after 10 h of pumping, such as the one used for the vessel, of $q_{des} \approx 3 \times 10^{-10}$ mbar l/cm^2 s [5]. As the furnace walls are cooled and don't exceed a temperature above 80 °C, we never baked the steel in a meaningful way.

Sample Run

The first run with samples was an 800 °C outgassing run, in which two Nb sample, which both underwent a coarse chemistry, were installed.

The temperature curve is shown in Fig. 6 and the respective pressure curve in Fig. 7. The starting pressure was 1.9 ×

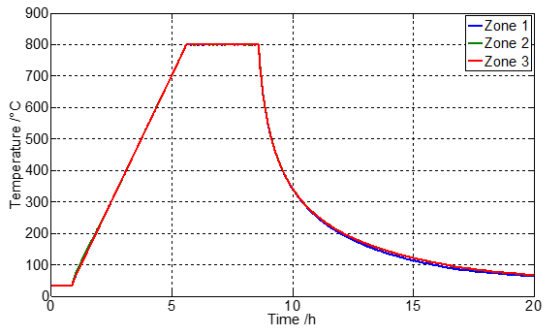

Figure 6: Temperature vs. time for the three heating zones for an outgassing run at 800 °C.

10^{-8} mbar and the maximum pressure of 5.7×10^{-7} mbar was reached at the beginning of the 800 °C plateau. The in-

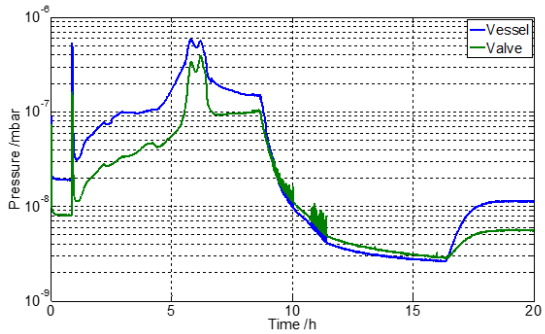

Figure 7: Pressure vs. time within the vessel (blue) and the corner valve (green) for the furnace run shown in Fig. 6. The spike at 1 h is caused by the start of the heating. The increase at approx. 16 h is due to the cooling water getting heated, causing desorption from the furnace walls.

crease of the pressure around 5 h is dominated by an increase of the pressure inside the corner valve. As the valve plate is heated up by heat radiation, it starts to desorb water stuck to the surface. The corresponding trendlines of various partial pressures are shown in Fig. 8. As expected, a rise of the water partial pressure around 6 h is seen.

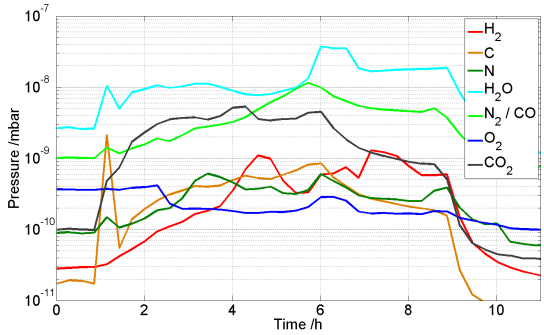

Figure 8: Partial pressure vs. time for selected masses. The spikes at 1 h are caused by the start of the heating.

The small peak in the hydrogen partial pressure after 4-5 h is due to the outgassing of H_2 from the niobium sample at 450 °C.

Sample Results

One of the samples was used to measure the RRR before and after the treatment while the other was used for SEM and SIMS analysis. The RRR measurement after the 800 °C run showed an increase, as it was 312 ± 5 before and 347 ± 5 after the run. A survey of the sample surface with a SEM showed no formation of carbides or other pollution, see Fig. 9.

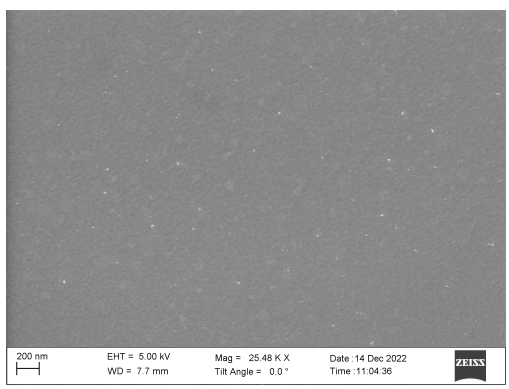

Figure 9: SEM image of the Nb sample after the outgassing run at 800 °C. No niobium carbides or other precipitates are observed.

The subsequent SIMS measurement of the niobium sample also showed no interstitial carbon down to the resolution of the system, see Fig. 10.

From those results, we conclude that the furnace, albeit the hydrocarbon signals above mass 45 in the RGA, does not contaminate Nb surfaces. Hence, as a next step, we decided to anneal a cavity.

FIRST CAVITY TREATMENT

The first cavity chosen to be annealed is 1DE10, a 1.3 GHz single-cell cavity which was coated with 18 nm Al_2O_3 prior to the annealing [6]. The cavity underwent the cleanroom preparation and had the baseline rf test at 2 K. Afterwards it was brought to and disassembled in the cleanroom, received one high pressure rinse and was then transported to

ISBN: 978-3-95450-234-9 ISSN: 2673-5504 doi:10.18429/JACoW-SRF2023-WEPWB111

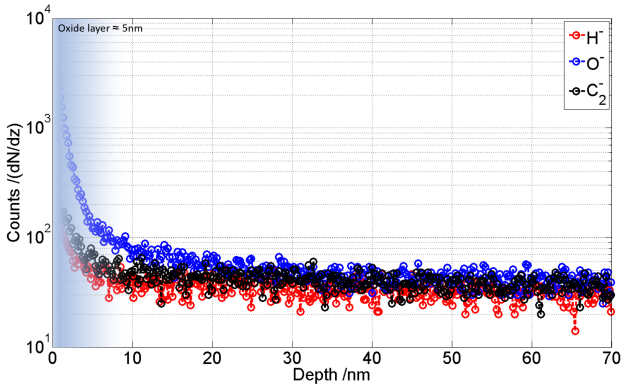

Figure 10: Counts vs. sputter depth obtained by a SIMS measurement for the Nb sample after the outgassing run at 800 °C. No interstitial carbon is detected.

the furnace. The cavity underwent a mid-T heat treatment, where the furnace temperature and pressure are shown in Fig. 11. Afterwards, the cavity was transported to the clean-

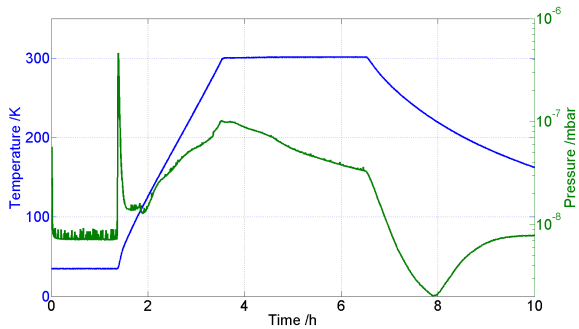

Figure 11: Temperature (blue) and pressure of the vessel (green) vs. time for the 1DE10 annealing. The pressure at the start of the heating was 7×10^{-9} mbar and the maximum pressure was 1×10^{-7} mbar.

room and underwent the preparation for the rf test. The rf test is shown in Fig. 12. The cavity itself showed a reduced

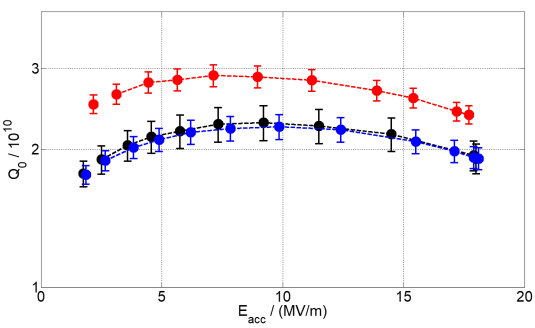

Figure 12: Quality factor vs. accelerating field of 1DE10. The lines are only to guide the eye. The 2 K measurements (black/blue) and the 1.8 K measurement is shown (red).

quench field of 18 MV/m, which is below typical quench fields of mid-T heat treated cavities. The same is found for the quality factor, which is significantly lower compared to other mid-T heat treated cavities. Yet, no field emission was observed, indicating that the handling and annealing did not cause a particle contamination. The next steps in the analysis will be to include temperature sensors at the charge during furnace runs, to monitor the cavity temperature during the runs. A smaller thermal budget, meaning the integrated area in the temperature-time plot, causing a not optimal diffusion process could explain this RF behaviour. This can only be identified by monitoring the temperature of the cavity during the run, and not only the furnace temperature.

SUMMARY

A new single-cell furnace dedicated for SRF R&D was designed and is now in operation. All specifications were achieved, yet an unwanted hydrocarbon contamination of the furnace, probably caused by a wrongfully installed component, is evident, but does not seem to pollute any niobium surfaces due to their low partial pressure level. This was concluded from the fact that all samples annealed so far in the furnace showed no carbon contamination. The first annealing of a single-cell cavity, namely 1DE10, was done using the mid-T heat treatment recipe. The cavity itself underperformed compared to other cavities treated with the same recipe, which shows that further diagnostics is needed, and a temperature sensor at the charge is necessary.

ACKNOWLEDGEMENTS

This work would not be possible without the excellent support by DESY (Hamburg, Germany), a member of the Helmholtz Association HGF. The authors would like to thank Uwe Lohse, Marcus Ortloff and Leo Amon (all at Xerion) for their excellent collaboration. This work was supported by the BMBF under the research grants 05K19GUB, 05H21GURB2 and 05K22GUD.

REFERENCES

[1] G. J. Thomas and W. Bauer, “Carbide formation on Nb surfaces during high–temperature H irradiation”, *J. Vac. Sci. Technol.*, vol. 12, no.1, pp. 490-495, 1975. doi:10.1116/1.568570

[2] M. Wenskat *et al.*, “Nitrogen infusion R&D at DESY a case study on cavity cut-outs”, *Supercond. Sci. Technol.*, vol. 33, no. 11, p. 115017, 2020. doi:10.1088/1361-6668/abb58c

[3] A. Dangwal Pandey *et al.*, “Grain boundary segregation and carbide precipitation in heat treated niobium superconducting radio frequency cavities”, *Appl. Phys. Lett.* vol. 119, no. 19, p. 194102, 2021. doi:10.1063/5.0063379

[4] J. W. Angle *et al.*, “Analysis of furnace contamination on superconducting radio frequency niobium using secondary-ion mass spectrometry”, *J. Vac. Sci. Technol., B*, vol. 41, no. 3, 2023. doi:10.1116/6.0002624

[5] P. Chiggiato, “Outgassing properties of vacuum materials for particle accelerators”, *arXiv*, 2020. doi:10.48550/arXiv.2006.07124

[6] G.K. Deyu *et al.*, “Successful Al2O3 coating of superconducting niobium cavities by thermal ALD”, presented at the SRF’23, Grand Rapids, MI, USA, Jun. 2023, paper MOPMB016, this conference.